JOURNAL OF SPACECRAFT AND ROCKETS
Vol. 49, No. 3, May–June 2012

Development of Electron-Emitting Film for Spacecraft Charging Mitigation

Minoru Iwata,* Arifur R. Khan,† Hideyuki Igawa,‡ Kazuhiro Toyoda,§ and Mengu Cho¶
Kyushu Institute of Technology, Fukuoka, 804, Japan
and
Tatsuhito Fujita**
Japan Aerospace Exploration Agency, Tokyo, 182, Japan

DOI: 10.2514/1.50735

Prevention of spacecraft charging and discharging has become increasingly important as geostationary Earth-orbit satellites employ higher bus voltages. There are numerous mitigation techniques against spacecraft charging, including electron emission from the spacecraft chassis. A new electron emission device operating in a completely passive manner has been developed, which uses the field enhancement at the triple junction where the interface of metal and insulator is exposed to space. It has been named electron-emitting film for spacecraft charging mitigation (ELF'S CHARM). Microetching was applied to polyimide-copper laminated film to manufacture a laboratory prototype. This prototype ELF maintains the emission current at the steady state from the triple junctions instead of leading to arcing. The electric field at the triple junction is macroscopically enhanced by charging the polyimide film and microscopically by dielectric impurities on the copper surface. The laboratory experiments confirmed a stable current emission from 10 to 100 μA for 4 hr from a 5-mm square sample having a 500-μm microetching pattern. Recently, the endurance of this ELF design has been confirmed by 100 hr of accumulated emission testing.

Nomenclature

ΔV = voltage difference across insulator, V
ϕ_{CG} = surface insulator (cover glass) potential, V
ϕ_S = spacecraft chassis potential, V

I. Introduction

SINCE the end of the 1990s, geostationary Earth orbit (GEO) satellites have increased in size dramatically. Nowadays, a power level of 10 kW is very common among commercial GEO telecommunication satellites. To sustain such high power generation requires a bus voltage over 100 V to decrease cable mass and to increase electrical power transmission efficiency. However, the risk of a power system failure increases with an increase in bus voltage.

Electrostatic discharge (ESD) on the surface of spacecraft, especially on solar arrays, has been one of the primary causes of on-orbit power system failures in spacecraft. ESD occurs when the spacecraft body potential becomes highly negative with respect to the ambient plasma as the flux of energetic electrons increases significantly due to encounters with substorms or aurora. When surface insulators, such as a solar array coverglass, have a positive potential with respect to the spacecraft chassis potential, i.e., inverted potential gradient, by several hundred volts, an ESD can occur easily. The temporal profiles of the spacecraft body and surface insulator are schematically shown in Fig. 1. If we can maintain the spacecraft body potential close to the ambient plasma potential, even when a spacecraft encounters a substorm or aurora, we can greatly reduce the risk of an ESD on the spacecraft surface.

In the present work, we have developed a device that emits electrons via field emission from a so-called triple junction, where the interface of the insulator and conductor are exposed to space plasma. We named it electron-emitting film for spacecraft charging mitigation (ELF'S CHARM). ELF is made by microetching metal-polymer laminate film that is less than 100 μm thick. Each ELF is several centimeters in size, and they are glued all over the surface of the spacecraft, using a conductive adhesive so that the conductive part has the same potential as the spacecraft chassis. The number of ELFs required to mitigate the charging of a typical large GEO telecommunication satellite is 100 or less, depending on the satellite's size and orbit. There have been various ideas presented to prevent spacecraft charging by emitting charged particles from the spacecraft body [1–3]. ELF has many advantages over the previously proposed method. First of all, it is capable of completely passive operation. It does not require any power source, as the power is provided by the electric field generated by the surface charging and absolute capacitance due to charging of the spacecraft with respect to the ambient plasma. It does not require any sensors to initiate its operation, as the surface charging automatically starts the field emission. It does not even require a wire harness. Therefore, it is easy to install, and the design change to present satellites is expected to be very minor. It also does not require any gas to generate electrons. Because it is made of a thin film, the total mass increase for a satellite is only 10 g or less, so severe satellite design changes are not necessary. The purpose of the present paper is to introduce the most recent developments of this ELF.

II. Theoretical Background

When a spacecraft body experiences negative charging, the electric field at the triple junction increases due to charging of the insulator surface. If the electric field exceeds a certain level, ESD can occur at the triple junction. The idea behind the operation of ELF is for this device to emit electrons via field emission before the field intensification can proceed on different parts of the spacecraft, such

Presented as Paper 2009-560 at the 47th AIAA Aerospace Sciences Meeting including The New Horizons Forum and Aerospace Exposition, Orlando, FL, 5–8 January 2009; received 13 May 2010; revision received 14 October 2011; accepted for publication 17 October 2011.

*Assistant Professor, Department of Applied Science for Integrated System Engineering, 1-1 Sensui, Tobata, Kitakyushu; iwata@ele.kyutech.ac.jp (Corresponding Author).
†Postdoctoral Researcher, 1-1 Sensui, Tobata, Kitakyushu.
‡Graduate Student, 1-1 Sensui, Tobata, Kitakyushu.
§Associate Professor, Department of Electrical Engineering and Electronics.
¶Professor, Department of Applied Science for Integrated System Engineering, 1-1 Sensui, Tobata, Kitakyushu. Senior Member AIAA.
**Associate Senior Engineer, Innovative Technology Research Center, 7-44-1 Jindaiji-Higashi, Chofu.

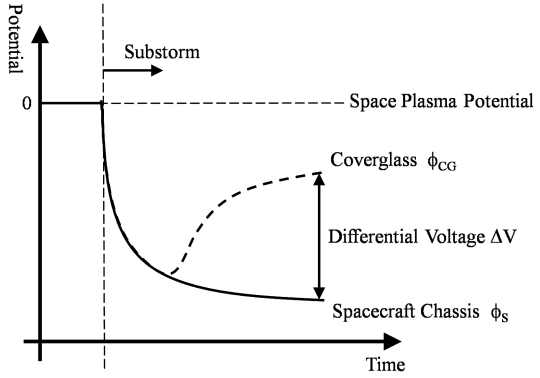

Fig. 1 Spacecraft potential profile during substorm in GEO.

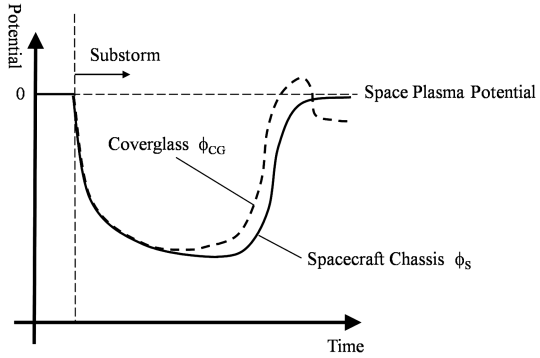

Fig. 2 Prospective view of spacecraft potential profile with an electron emitter during substorm in GEO.

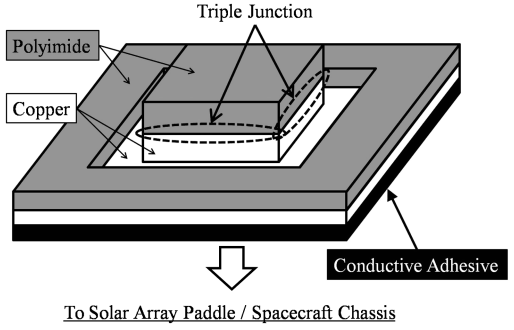

Fig. 3 Schematic picture of ELF device.

as the solar array coverglass. The electron emission raises the spacecraft body potential to nearly zero, as schematically shown in Fig. 2. This makes the spacecraft insulator surface negatively charged with respect to the body, producing a so-called normal potential gradient, where the ESD inception threshold is 10 times higher than the inverted potential gradient. Electron emissions from the triple junction exposed to the environment have been shown to be a precursor phenomena to ESD. The new device uses this precursor phenomena but maintains emissions up to a level that prevents transition to ESD.

Figure 3 shows a schematic picture of the ELF under development. As the geometry is not optimized yet, the ultimate product may have a different shape; however, the basic elements will be the same. ELF consists of a thin film of insulation (polyimide) on top of a copper substrate, which exposes part of the metallic substrate. It is glued by conductive adhesive to the conductive surface, which is connected to the satellite body. When the ELF is exposed to energetic electrons, the metallic part has the same potential as the satellite chassis. The insulator surface can have a different potential from that of the satellite chassis because of the secondary electron emission. By selecting the proper material with a high secondary electron emission coefficient, we can make the insulator potential more positive than the chassis potential. This state is called an inverted potential gradient. Once the electric field builds up due to the inverted potential gradient, the highest electric field is formed at the triple junctions, where the conductor, insulator, and vacuum meet, as shown in Fig. 3. In Fig. 3, the typical thickness of the polyimide is 3 μm. The height of the square-shaped copper protrusion at the center is typically 10 μm. The width of the center protrusion varies from 100 μm to 3 mm in the present paper. If there is any dielectric impurity on the metal surface, we can expect the local enhancement of the electric field up to several thousand times [4]. This is due to the direct input of electrons from the metal surface to the conduction band of the dielectric impurity. Electrons are accelerated inside the conduction band and produce holes via ionization. The holes migrate toward the metal-dielectric interface and further enhance the electric field while the electrons are emitted from the dielectric-vacuum interface.

Once the field emission starts from the triple junctions, we can expect further enhancement of the current by charging of the insulator near the emission site. Some of the field-emitted electrons hit the insulator surface and induce secondary electron emission, as shown in Fig. 4. If more than one secondary electron is emitted by one incident electron, a positive charge is left on the insulator surface. The positive charge further enhances the electric field on the metal surface. Higher numbers of field emission electrons induce even more secondary electrons, and eventually, the emission current shows avalanchelike behavior because the field emission current is an exponential function of the electric field. After the avalanche is set off, the negative charge of the field-emitted electrons eventually limits the field emission current. The space charge limitation

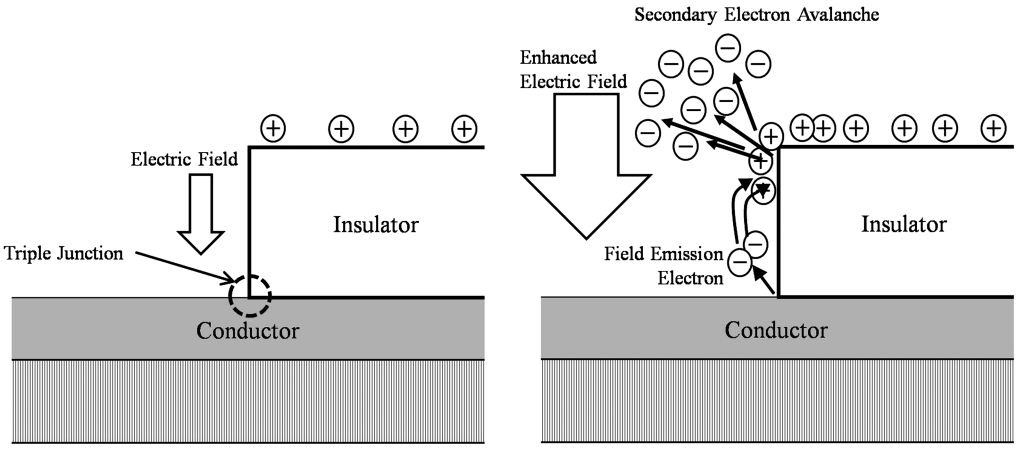

a) Formation of electric field at the triple junction **b) Field emission and secondary electron avalanche**

Fig. 4 Schematic microscopic picture of a triple junction, showing the electric field, field emission, and secondary electron avalanche.

eventually saturates the field emission current. The described mechanism of field enhancement near the triple junction was proposed as a prebreakdown mechanism for a high-voltage solar array arcing in the early 1990s [5,6].

ELF uses the prebreakdown mechanism of arcing at the triple junction on high-potential spacecraft. An arc occurs on the spacecraft due to the continuous bombardment of field emission electrons on the insulator surface even after saturation of the field emission current. This continuous bombardment of electrons also ionizes the neutral gas molecules desorbing from the surface via electron impact.

III. Experiment

A. Test Sample

Figure 5 shows a microscopic photograph of a typical testing ELF containing a triple junction. The area between two concentric squares is the exposed metallic part, and the remaining areas are covered by polyimide. The dimensions of the inner area are 500×500 μm, while characterizes the ELF by name. The geometry of each square is shown in Fig. 3. These square patterns were made by microetching on a polyimide-copper laminated plate. We made four types of emitters, differing by the size of the inner square: 3×3 mm, 1×1 mm, 500×500 μm, and 100×100 μm, as shown in Fig. 6. The area without any pattern is plain polyimide film on the copper substrate, which is used to measure the insulator surface potential by a noncontacting surface potential probe during the experiment. These emitters were stored in a desiccator until the experiment was started in a vacuum. Before starting the evacuation, each coupon was placed individually on glass after adding a 10 MΩ resistor. After a satisfactory vacuum was established, the experiment was started.

B. Experimental Facility

Figure 7 shows a schematic picture of the experimental setup. All ELF coupon experiments were performed in a vacuum chamber that had a cylindrical shape of 600 mm in diameter and 900 mm in length, which was evacuated by a turbo molecular pump to achieve a pressure of $\sim 2.0 \times 10^{-4}$ Pa. The chamber was also equipped with an electron gun (OME-0050LL). We irradiated the ELF surface with electrons from the gun to simulate the substorm condition that boosted the inverted potential gradient on the ELF surface. The two-dimensional (2-D) distribution of surface potential on the ELF surface was measured by a noncontacting surface potential probe (Trek model 341B) attached to the XY stage controller unit (Sigma-Koki SGSP26-150 and SGSP26-200). The chamber was also equipped with an infrared camera (Sony XC-E150) to detect the location of luminescence due to electron emission and/or discharge. To simulate a negatively charged spacecraft with respect to the ambient plasma on which the ELF was glued, we biased the ELF to a negative potential using a variable direct current (DC) power supply (V_{bias}). Figure 8 shows a schematic picture of the present electrical circuitry and the data acquisition system for the performance test. A 10 MΩ resistor (R) was attached to each ELF to simulate the resistance of the conductive adhesive on the satellite body. Another 10 MΩ resistor (Rs) was used to protect the DC power supply from damage caused by any short circuit. A capacitor of 300 pF was set in the external circuit to simulate the spacecraft capacitance as well as to increase the discharge current to a detectable amount when it occurs. The DC current probes Cp1 and Cp2 (Hioki 3272) were used to measure the arc current. During electron emission from the ELF surface, there was a potential drop that was monitored by using a high-voltage probe, Vp (Agilent N2771A), and was used to derive the emission current from the voltage drop across the resistor Rs.

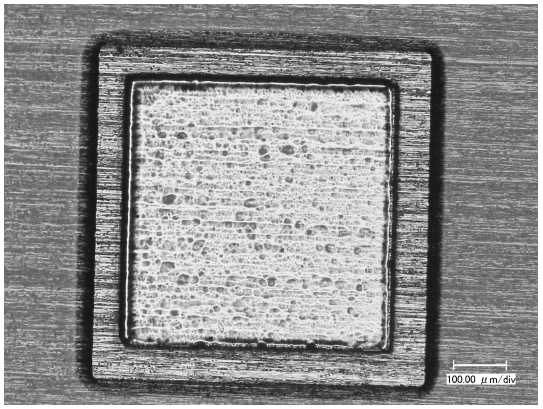

Fig. 5 Microscopic photograph of an ELF coupon with a typical 500 × 500 μm square.

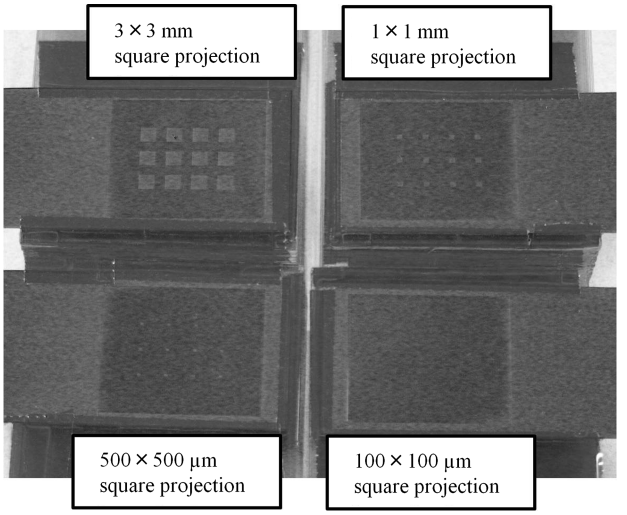

Fig. 6 Photograph of an ELF coupon with various square sizes.

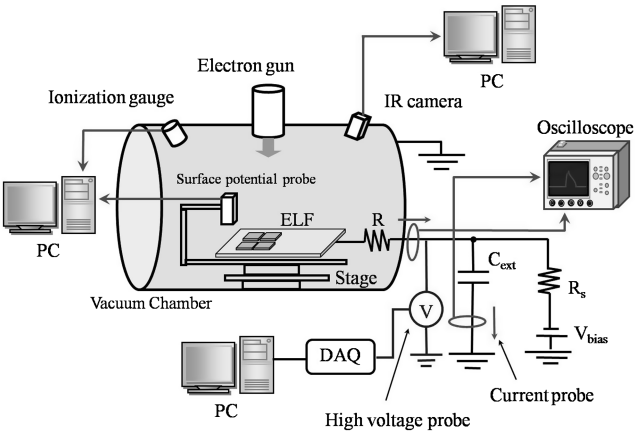

Fig. 7 Schematic diagram of experimental setup for performance test.

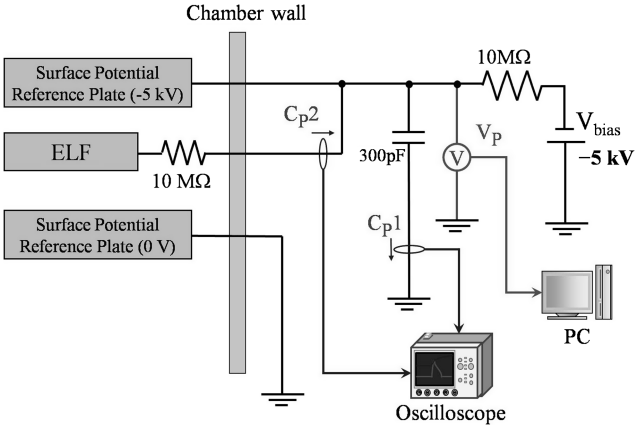

Fig. 8 Schematic diagram of the electrical circuitry and data acquisition system in the performance test.

During the electron emission, often an anomalous sharp rise in the emission current was detected by a high-voltage probe. Sometimes, during the emission, an optical luminescence was also detected by the infrared camera on the ELF surface.

IV. Results and Discussions

A. Emission Performance Test

To check the emission performance of ELF, it was irradiated with an electron beam with an energy level of 5.2 keV and a current of 50 μA to make the surface a positive potential with respect to the sample bias of −5.0 kV. By selecting the proper electron beam parameters, an inverted potential gradient was generated that created a field emission from the triple junctions in several of the squares (there are 12 squares on the ELF surface; however, the emission point is still unknown) on the ELF surface. Figure 9 shows the emissions from four types of ELF. In the figure, we mark the time when discharges were detected. The discharge occurs when the emission current deviates from a stable level and runs away by quickly increasing by orders of magnitude. The discharge at ELF is not a concern in orbit as it occurs at places much safer than the critical components, such as the solar array. It can also neutralize the charging process over the solar array around ELF [7]. The detrimental effect of discharge on ELF in orbit is probably limited to electromagnetic interference. Although we see occasional discharges, an average of 40 to 50 μA is observed throughout Fig. 9, which means the emission current does not depend on the projection size. This is reasonable, considering the nonlinear nature of field emissions and localized emission sites on the metal surface [4]. It is possible that an emission from one site dominates the other sites, in which case the size of projection does not matter.

Figure 9 also shows frequent drops in the emission current as well as sudden jumps that are not associated with discharge. Because ELF operates in a group distributed over the whole of the spacecraft surface, a drop in the current of one ELF does not degrade the overall performance. As long as the total emission current from all the ELFs on the spacecraft balances the total current of incoming energetic electrons, the spacecraft body potential can be maintained near zero. The sudden jump in the current was detected with an additional oscilloscope whose time range was much larger than the time range

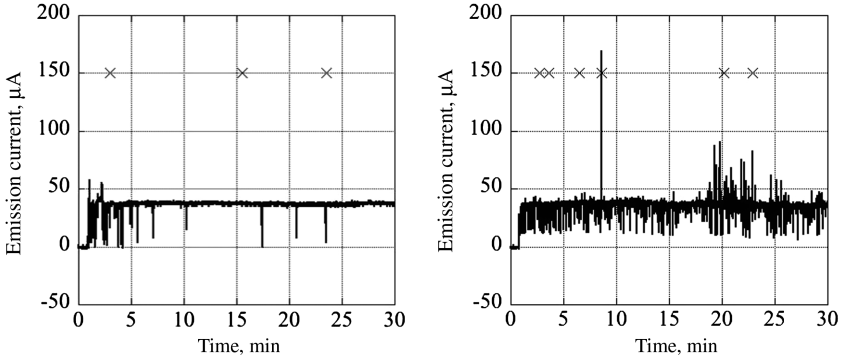

a) 100 × 100 μm square ELF b) 500 × 500 μm square ELF

c) 1 × 1 mm square ELF d) 3 × 3 mm square ELF

Fig. 9 Emission current from various ELF during performance tests. The discharge time is indicated by the "×".

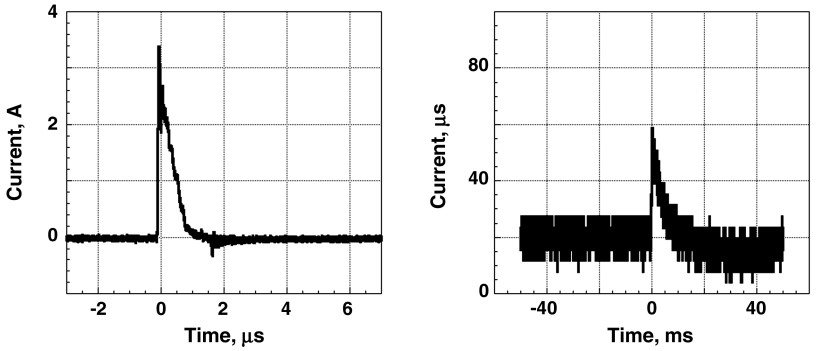

a) Current waveform of discharge b) Sudden jump in the emission current

Fig. 10 Comparison of sudden jump in the emission current with discharge current.

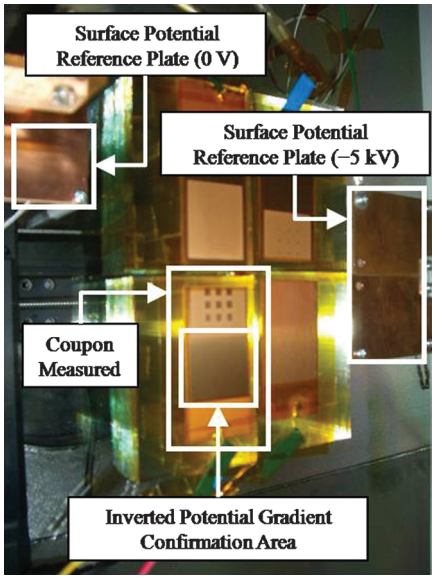

Fig. 11 ELF and reference plates arrangement inside vacuum chamber during surface potential measurement.

of the main oscilloscope, which was used to measure the discharge waveform. One example of a typical discharge current and a sudden jump in the emission current is shown in Figs. 10a and 10b, respectively. The former has a pulse width of approximately 10 μs, and its peak value is 3.5 A, as shown in Fig. 10a. The latter has a time scale around 100 ms. In the present paper, this sudden jump in the emission current is called a rapid electron emission (REE) to distinguish it from the discharge. The cause of REEs is currently not clear; however, details of the phenomena may be explained in the near future. Again, because ELF operates as a group, a REE at one ELF does not affect the overall performance of the group.

To confirm the inverted potential gradient, the potential of the polyimide-covered ELF inside the vacuum chamber was measured. A bias voltage of −5 kV was applied to the substrate, followed by irradiation with an electron beam of 5.2 keV and 50 μA to the polyimide-covered ELF surface for 5 min. After shutting the beam off, the area shown in Fig. 11 was immediately scanned. Figures 12a and 12b show the potential distribution of this area before and after the electron beam irradiation, respectively. The reference potential plates of −5 kV and 0 V are clearly shown on the far right and in the top left corner, respectively. The biased coupon showed color similar to the reference plate of −5 kV. The square area marked by black lines corresponds to the plain polyimide surface without any exposed metal substrate and has more positive potential than −5 kV by approximately 1 kV. Therefore, it was confirmed that an inverted potential gradient condition exists over the 12 squares where there are triple junctions.

The emission current increased with an increase of the potential difference between the insulator surface and the metallic part. The insulator surface potential is determined by the balance of secondary electrons and incident electrons. The electrons having energy of 200 eV hit the ELF surface, which has a −5 kV bias, when the electron beam energy is 5.2 keV. At this incident energy, the secondary electron emission coefficient of polyimide (the surface materials of ELF) is larger than unity, as shown in Fig. 13, which shows the energy dependence of secondary electron emission yield on a polyimide Kapton, based on a model [8] and experimental data [9,10]. Because the number of secondary electrons is larger than that of the incident electrons, the insulator surface creates a positive potential greater than −5 kV. At the same time, the incident electron energy on the insulator surface increases with the increase of the insulator surface potential. For example, if the surface potential increases around −4.5 kV, while being irradiated with an electron beam of 5.2 kV, the incident electron energy on the insulator surface rises to around 700 eV. As shown in Fig. 13, the secondary electron emission coefficient is larger than unity when the incident electron energy is between 20 and 680 eV. Therefore, if the surface potential increases to −4.5 kV, the potential difference between the insulator surface and the metallic part does not continue to increase due to the balance of secondary and incident electrons. To simulate further potential differences between the insulator surface and the metallic part, the incident electron energy should be controlled on the insulator surface to within the range of 20 to 680 eV due to the reduction of electron beam energy. By varying the beam energy, the insulator surface potential can be controlled. The way the emission current varies due to changes of the beam energy during the experiment is shown in Fig. 14. The bias voltage of the ELF substrate was kept to −5 kV, and only one 3 × 3 mm square was exposed to the electron beam, whereas the rest of the surface was covered by polyimide tape. First, we used a beam energy of 5.5 keV. The emission current was restarted after 48 min and stabilized for several minutes; after which the beam energy was lowered to 4.8 keV, and the emission current jumped to 70 μA. The beam energy was further

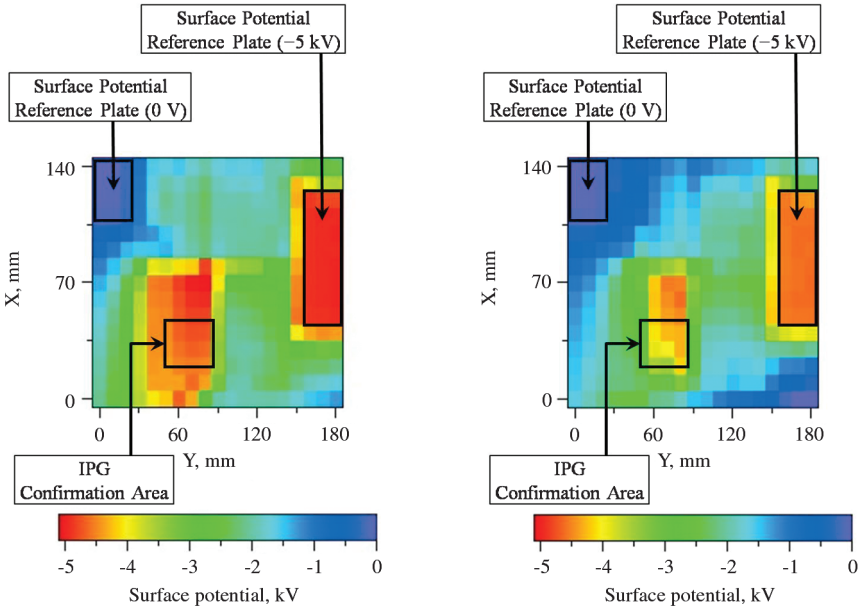

a) Before electron beam irradiation **b) After electron beam irradiation**

Fig. 12 2-D potential distribution on ELF surface and reference plates.

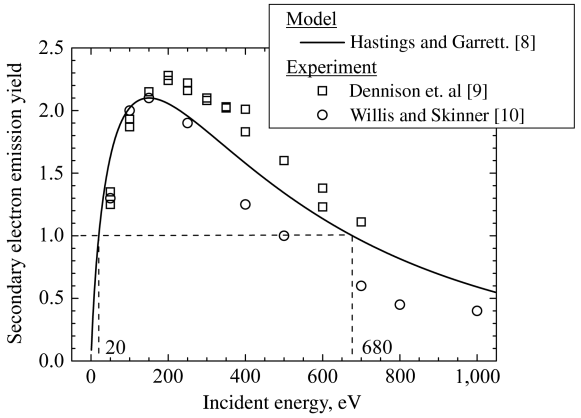

Fig. 13 Energy dependence of secondary electron emission yield on a polyimide Kapton, based on a model [8] and experimental data [9,10].

decreased to 3 keV, and this pattern continued, as shown in Fig. 14. After 61 min, the beam was shut off, and the emission was stopped. The emission occurred even with 3 keV beam energy, which means that the insulator potential was more positive than −3 kV and ensured that the inverted potential gradient was greater than 2 kV during the field emission under the electron beam irradiation.

B. Endurance Test

A typical GEO satellite encounters substorm conditions for 12 hr per year during sun-lit conditions [11]. If we include eclipses, it is 34 hr. Over the 15 years of a typical operational lifetime, the total duration of substorm conditions is 500 to 600 hr. Therefore, we have to demonstrate that ELF could continue to operate effectively even after 600 cumulative hours using a ground test. To check the emission performance under substorm conditions over a long time period, a 100-hr (accumulated) endurance test was performed under the same conditions mentioned in Section IV.A. The experimental results are shown in Fig. 15. Although discharges and REE were observed during the electron emission, the ELF device continued to function until we shut the beam off and stopped the sample bias. We have confirmed that ELF can operate for a period of time longer than 100 hr.

In our studies to date, the typical emission current from one pristine ELF coupon at the beginning of operation was observed around 40 to 50 μA. Suppose the total surface area of a GEO satellite is 400 m^2 and an energetic electron current density of 10 μA/m^2 during a substorm in space [11], then the total electron current incoming to the satellite is 4 mA. Therefore, if the satellite has 100

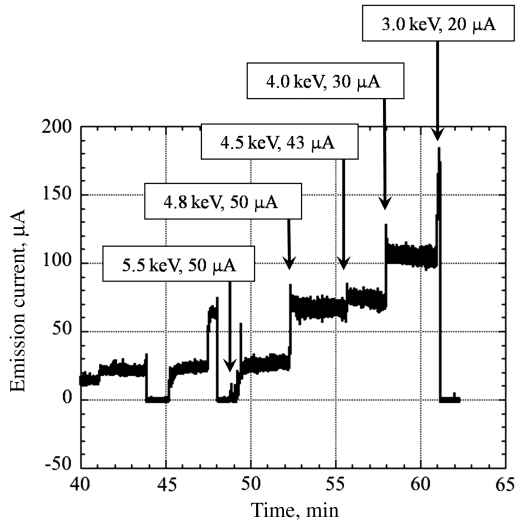

Fig. 14 Effect of electron beam energy on emission current.

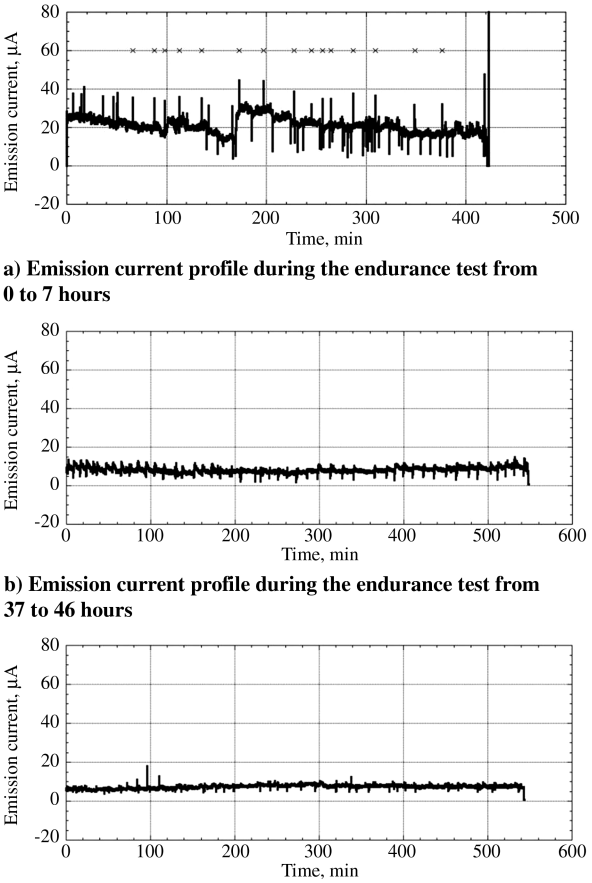

a) Emission current profile during the endurance test from 0 to 7 hours

b) Emission current profile during the endurance test from 37 to 46 hours

c) Emission current profile during the endurance test from 91 to 100 hours

Fig. 15 Emission current from ELF during endurance tests. The discharge time is indicated by "×".

ELFs and each operates satisfactorily, the energetic electron current can be balanced by the ELF emission current.

The current development goal for ELF is to achieve technical readiness level 6 and prepare it for an orbital demonstration. There are six parts of this goal:

1) Theory: A theoretical value of the emission current should be derived based on a model of physical processes leading to the start of electron emission to explain the experimental results.

2) Design optimization: Fig. 3 shows the present design of ELF. This geometry is not necessarily optimized for the maximum emission current. The numerical simulations, design, manufacture, and testing to reach the optimized shape need to be repeated.

3) Yield rate: Mass production of ELF using microetching technology of polyimide-copper laminated film should be the goal. ELFs will be distributed over the whole satellite surface, so that the performance of each ELF should be uniform; ideally, the electron emission pattern of every ELF should be tested. The emission performances of many samples should be measured to improve the yield rate within an acceptable range. In the performance measurement, the electron emission under nonmonoenergetic electron bombardment should also be measured.

4) Environmental durability: It must be demonstrated that ELF can withstand exposure to such conditions as radiation, ultraviolet rays, and thermal cycle.

5) Optimum distribution pattern: The distribution of ELF over the satellite surface should be analyzed. The insulator surface on a satellite has different charging potentials depending on its location in space. So, depending on the satellite's orbit and location, the optimum pattern of ELF distribution over the satellite needs to be studied further. By using the multi-utility spacecraft charging analysis tool (MUSCAT) [12], we were able to solve the surface charging potential distribution. This software can also be used to

understand how the spacecraft chassis potential is neutralized by the electron emission due to ELF on the spacecraft. The potential-barrier effects that may prevent field-emitted electrons from escaping are automatically included in the simulation.

6) Material optimization: The current design of ELF uses a combination of copper and polyimide. More efforts are underway to improve the performance by using an insulator material that has a higher secondary electron emission yield.

V. Conclusions

In this paper, the development status of ELF'S CHARM is described. Microetching was applied to thin polyimide-copper laminate film to produce a metal-exposed area over the surface at triple junctions. ELF uses the prebreakdown mechanism of arcing on a solar array under an inverted potential gradient. Because the polyimide is more positively charged than copper, electrons are emitted via field emission from the copper. The laboratory experiments demonstrated that each ELF is capable of emitting a stable current up to 100 μA or even higher while exposed to an electron beam. It has been demonstrated that the emission current depends on the potential difference across the insulator because it was possible to control the emission current by varying the insulator surface potential by shifting the electron incident energy to change the secondary electron emission yield from the polyimide. It was also demonstrated that the long-term operation of ELF could exceed 100 hr. Suppose the total surface area of a GEO satellite is 400 m^2, and the total electron current incoming to the satellite is 4 mA. Therefore, if the satellite has 100 ELFs and each operates satisfactorily, the energetic electron current can be successfully balanced by the ELF emission current. The current balance maintains the potential of the satellite body near zero, which is the normal potential gradient, and greatly reduces the risk of discharge inception.

The current development goal of ELF is to achieve technical readiness level 6 and make it ready for orbital demonstration. The progress made on each research item will be reported in the near future. In an orbital demonstration, the functioning of ELF in a natural environment will be exposed to the full range of electron energy spectrum and will test the prevention of spacecraft charging by returning electrons from the spacecraft chassis to the surrounding plasma, even in the presence of a complex potential barrier around the spacecraft.

Acknowledgments

This work was supported by Grant in Aid for Scientific Research (A) no. 19206090 of the Japan Society for the Promotion of Science, the Seeds Development Experiment Grant of the Japan Science and Technology Agency and the Space Open Laboratory Grant of the Japan Aerospace Exploration Agency (JAXA). We are grateful to T. Sumida, K. Saito, Y. Fujiwara, T. Yamamoto, Y. Sanmaru, T. Okumura, and S. Hosoda for supporting the experiments; to R. Shiratsuchi of the Kyushu Institute of Technology for supporting the surface roughness measurements, S. Hatta of MUSCAT Space Engineering for supporting the numerical simulations, T. Sato and Y. Mizuguchi of Molex Kiire Co. Ltd. for providing the ELF devices, and Y. Ohkawa, K. Koga, T. Watanabe, and Y. Hisada of JAXA for discussing the results.

References

[1] Cooke, D., and Geis, M., "Introducing The Passive Anode Surface Emission Cathode," *38th AIAA/ASME/SAE/ASEE Joint Propulsion Conference & Exhibit*, AIAA Paper 2002-4049, Indianapolis, IN, 2002.

[2] Mandell, M. J., Davis, V. A., Gardner, B. M., Wong, F. K., Adamo, R. C., Cooke, D. L., and Wheelock, A. T., "Charge Control of Geosynchronous Spacecraft Using Field Effect Emitters," *45th AIAA Aerospace Sciences Meeting and Exhibit*, AIAA Paper 2007-284, Reno, NV, 2007.

[3] Dichter, B. K., Ray, K. P., Gussenhoven, H.S., Holeman, E.G., Delorey, D. E., and Mullen, E. G., "High Voltage Frame and Differential Charging Observed on a Geosynchronous Spacecraft," *6th Spacecraft Charging Technology Conference*, AFRL VS-TR-20001578, Air Force Research Laboratory Science Center, Hanscom Air Force Base, MA, 2000.

[4] Latham, R. V., "Origin of Prebreakdown Electron Emission from Vacuum-Insulated High Voltage Electrodes," *Vacuum*, Vol. 32, No. 3, 1982, pp. 137–140. doi:10.1016/0042-207X(82)80043-2

[5] Snyder, D. B., and Tyree, E., "The Effect of Plasma on Solar Cell Array Arc Characteristic," NASA TM 86886, 1985.

[6] Cho, M., "Arcing on High Voltage Solar Arrays in Low Earth Orbit: Theory and Computer Particle Simulation," Ph.D. Thesis, Massachusetts Inst. of Technology, Cambridge, MA, 1992.

[7] Masui, H., Toyoda, K., and Cho, M., "Electrostatic Discharge Plasma Propagation Velocity on Solar Panel in Simulated Geosynchronous Environment," *IEEE Transactions on Plasma Science*, Vol. 36, No. 5, 2008, pp. 2387–2394. doi:10.1109/TPS.2008.2003191

[8] Hastings, D., and Garrett, H., *Spacecraft Environment Interactions*, Cambridge Atmospheric and Space Science Series, Cambridge Univ. Press, Cambridge, England, U.K., 1996, pp. 150–151.

[9] Dennison, J. R., Sim, A., and Thomson, C. D., "Evolution of the Electron Yield Curves of Insulators as a Function of Impinging Electron Fluence and Energy," *IEEE Transactions on Plasma Science*, Vol. 34, No. 5, 2006, pp. 2204–2218. doi:10.1109/TPS.2006.883398

[10] Willis, R. F., and Skinner, D. K., "Secondary Electron Emission Yield Behavior of Polymers," *Solid State Communications*, Vol. 13, 1973, pp. 685–688. doi:10.1016/0038-1098(73)90459-6

[11] Cho, M., Kawakita, S., Nakamura, M., Takahashi, M., Sato, T., and Nozaki, Y., "Number of Arcs Estimated on Solar Array of a Geostationary Satellite," *Journal of Spacecraft and Rockets*, Vol. 42, No. 4, 2005, pp. 740–748. doi:10.2514/1.6694

[12] Muranaka, T., Hosoda, S., Kim, J., Hatta, S., Ikeda, K., Hamanaga, T., Cho, M., Usui, H., Ueda, H., Koga, K., and Goka, T., "Development of Multi-Utility Spacecraft Charging Analysis Tool (MUSCAT)," *IEEE Transactions on Plasma Science*, Vol. 36, No. 5, 2008, pp. 2336–2349. doi:10.1109/TPS.2008.2003974

T. Minton
Associate Editor